NOTES AND CORRESPONDENCE

On the Positive Bias of Peak Horizontal Velocity from an Idealized Doppler Profiler

DAVID A. SHORT

ENSCO, Inc., Cocoa Beach, Florida

FRANCIS J. MERCERET

Applied Meteorology Unit, NASA, Kennedy Space Center, Florida

(Manuscript received 20 January 2004, in final form 26 July 2004)

ABSTRACT

In the presence of 3D turbulence, peak horizontal velocity estimates from an idealized Doppler profiler are found to be positively biased due to an incomplete specification of the vertical velocity field. The magnitude of the bias was estimated by assuming that the vertical and horizontal velocities can be separated into average and perturbation values and that the vertical and horizontal velocity perturbations are normally distributed. Under these assumptions, properties of the type-I extreme value distribution for maxima, known as the Gumbel distribution, can be used to obtain an analytical solution of the bias. The bias depends on geometric properties of the profiler configuration, the variance in the horizontal velocity, and the unresolved variance in the vertical velocity. When these variances are normalized by the average horizontal velocity, the bias can be mapped as a simple function of the normalized variances.

1. Introduction

Doppler profilers are used to obtain estimates of horizontal (U) and vertical (W) velocity within the atmosphere (Van Zandt 2000) and underwater (Woodward and Appell 1986) using acoustic, radar, and optical remote sensing techniques. Electromagnetic or acoustic energy at a known frequency is transmitted into the medium of interest, and the frequency of the backscattered energy is measured by a directional receiver. Receiver characteristics such as size and shape define its beam, typically a narrow cone projecting away from the receiver throughout some depth of the fluid. The difference between the transmitted and received frequencies, referred to as the Doppler shift, is used to estimate the velocity component of backscatterers along the beam axis. The backscattering elements are assumed to be passive tracers of the fluid motion, and the estimated velocity component along the beam axis is referred to as the radial velocity (R). Sophisticated transmitter/receiver configurations and signal generating/processing techniques have been developed over the past several decades to maximize the accuracy of R estimates and subsequent retrieved U and W.

The average retrieved horizontal velocity ($\overline{U_{\mathrm{Ret}}}$) from Doppler profiling systems has been validated extensively with in situ observing systems in both the atmosphere (May et al. 1989; Crescenti 1997) and underwater (Chereskin et al. 1987; Gilboy et al. 2000). It is generally well estimated for averaging times of 15 min or greater. Average measures of turbulence, such as the turbulent kinetic energy, can also be derived from Doppler profiler observations by statistical/dynamical methods (Kramar and Kouznetsov 2002; Lu and Lueck 1999b). However, the precision of the retrieved instantaneous horizontal velocity $[(\overline{U} + u')_{\mathrm{Ret}}]$, where u' implies a perturbation from $\overline{U}$ with a time scale of a few seconds, is more problematic (Lu and Lueck 1999a). As a result, the accuracy of the retrieved peak horizontal velocity $[(U_n^{\Delta})_{\mathrm{Ret}}]$ from a collection of $(\overline{U} + u')_{\mathrm{Ret}}$ of size n can be significantly affected.

The present study was motivated by a field test of an acoustic profiler on Cape Canaveral Air Force Station (CCAFS) in which average and peak wind speed data were compared to anemometer observations from a tall wind tower [see Short and Wheeler (2003) for details]. Accurate measurement of peak wind speeds is important to the safety of space launch operations at CCAFS. There are peak wind speed constraints designed to pro-

Corresponding author address: David A. Short, ENSCO, Inc., 1980 N. Atlantic Ave., Suite 230, Cocoa Beach, FL 32931.
E-mail: short.david@ensco.com

© 2005 American Meteorological Society

tect a launch vehicle from wind stresses that could damage or topple it. Figure 1 shows that the average peak wind speeds from the profiler were systematically higher than those from the wind tower. In addition, the profiler bias in average peak wind speed tended to increase with an increase in the standard deviation of the vertical velocity (see Fig. 1), which peaked at about 1900 UTC (1500 LT) during the 2-week period of record. On the other hand, the average wind speeds (not shown) from the profiler and tower were within a few percent of one another. Although the retrieval algorithms used for the profiler were proprietary in nature, the consistent nature of the bias in the average peak wind speed and its apparent correlation with the variance of the vertical velocity, along with the profiler's unbiased estimate of average wind speed, have stimulated this effort to formulate a plausible explanation.

This paper describes an idealized Doppler profiler in an idealized fluid, where the true instantaneous radial velocity $[(\overline{R} + r')_{\text{True}}]$ is composed of weighted sums of $(\overline{U} + u')_{\text{True}}$ and $(\overline{W} + w')_{\text{True}}$, with weights dependent on the beam configuration. In the case of 3D turbulent flow, the typical beam configuration does not provide adequate information for an accurate estimate of $(\overline{U} + u')_{\text{Ret}}$, although its average, $\overline{(\overline{U} + u')_{\text{Ret}}}$, can be shown to be unbiased under certain assumptions. For applications where U_n^{Δ} from a collection of $\overline{U} + u'$ of size n is of interest, errors in $(\overline{U} + u')_{\text{Ret}}$ propagate into $(U_n^{\Delta})_{\text{Ret}}$ and, in general, introduce a positive bias in the average retrieved peak value $\overline{(U_n^{\Delta})_{\text{Ret}}}$. Section 2 describes an idealized profiler configuration along with retrieval algorithms for uniform and turbulent flows. Section 3 uses extreme value theory to provide analytical solutions to $\overline{(U_n^{\Delta})_{\text{Ret}}}$ and $\overline{(U_n^{\Delta})_{\text{True}}}$ as a function of turbulent properties of the fluid and the profiler configuration. Section 4 provides a summary and conclusions. A list of symbols is given in the appendix.

2. An idealized Doppler profiler

The following description of an idealized Doppler profiler is intended to represent, in the simplest terms, how $(\overline{U} + u')_{\text{True}}$ and $(\overline{W} + w')_{\text{True}}$ combine to form $(\overline{R} + r')_{\text{True}}$ from the oblique and vertical beams of a typical system. The $(\overline{R} + r')_{\text{True}}$ are then used to obtain $(\overline{U} + u')_{\text{Ret}}$. For conditions where $(\overline{W} + w')_{\text{True}}$ varies in space and/or time, $(\overline{U} + u')_{\text{Ret}}$ is shown to be susceptible to an error that is directly proportional to the difference in $(\overline{W} + w')_{\text{True}}$ over the oblique and vertical beams. A statistical modeling approach is used to show how this difference affects the overall average retrieved peak wind speed $\overline{(U_n^{\Delta})_{\text{Ret}}}$. The statistical model quantifies three important characteristics: 1) $(\overline{U} + u')_{\text{Ret}}$ is unbiased under reasonable assumptions, 2) $\overline{(U_n^{\Delta})_{\text{Ret}}}$ is positively biased under the same assumptions, and 3) the magnitude of the positive bias is dependent on the unresolved temporal and/or spatial variations of $(\overline{W} + w')_{\text{True}}$.

Consider an idealized Doppler profiler that measures $(\overline{R} + r')_{\text{True}}$ along each of two beams, b_1 and b_2, as in Fig. 2. The b_1 beam is vertically oriented with respect to the local horizontal plane. The b_2 beam is oriented at an angle Θ from the vertical in order to obtain information about U. While the typical Doppler profiling system has three or more beams to resolve the three orthogonal velocity components, the essence of the mathematical and statistical arguments supporting a positive bias in $\overline{(U_n^{\Delta})_{\text{Ret}}}$ can be readily developed for a two-beam system and are generally applicable for a multibeam system.

The profiler obtains doublets of $(\overline{R} + r')_{\text{True}}$, namely, $\mathbf{V}_1$ (D_1) and $\mathbf{V}_2$ (D_2), where the symbols D_1 and D_2

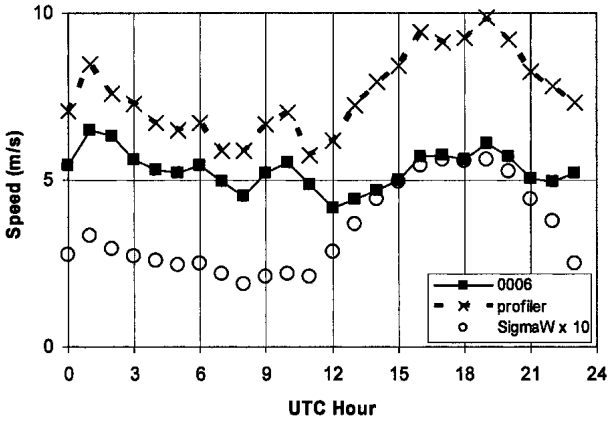

FIG. 1. Average peak wind speed values from the 60-m level of an acoustic profiler (x) and from the nearest corresponding level (62 m) of a nearby tall wind tower (■). The standard deviation of vertical velocity (o), multiplied by 10 and obtained from the vertical beam of the profiler, is also shown. Local time is given by the UTC hour minus 4.

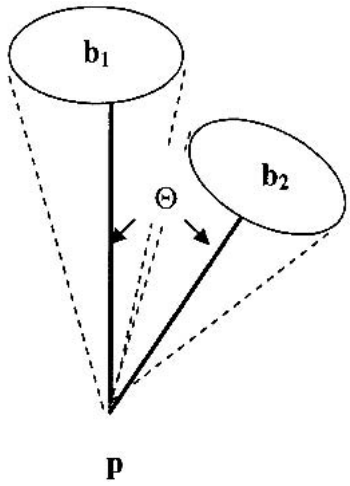

FIG. 2. Schematic of an idealized two-axis Doppler profiler system.

denote distances from point p in Fig. 2, the location of the instrument. The condition $D_1 = D_2 \cdot \cos(\Theta)$ is required to obtain radial velocities from both beams at the same height, $H = D_1$, above the local horizontal plane. The following notation was developed by assuming that this condition was met and dropping the notation for height and distance. Note also that Θ is typically about 15° for atmospheric systems and 30° for underwater systems in order to obtain profile information over a useful depth and to avoid b_2 sidelobe contamination from ground targets with zero-Doppler shift. Because Θ is small, $\mathbf{V}_2$ can be significantly affected by $(\overline{W} + w')_{\text{True}}$.

a. Equations for a uniform velocity field with no turbulence

Under idealized conditions of temporal and spatial uniformity in the velocity field, the idealized profiler observations are described by the following equations (Peterson 1988):

$$\mathbf{V}_1 = (W)_{\text{True}}, \tag{1}$$

$$\mathbf{V}_2 = (U)_{\text{True}} \sin(\Theta) + (W)_{\text{True}} \cos(\Theta). \tag{2}$$

Equation (2) can be directly solved for $(U)_{\text{True}}$ as follows:

$$(U)_{\text{True}} = \mathbf{V}_2 \sec(\Theta) - (W)_{\text{True}} \cot(\Theta). \tag{3}$$

There are three important points to note from Eqs. (1)–(3):

1) Equation (1) shows that $(W)_{\text{True}}$ is obtained from $\mathbf{V}_1$, the radial velocity measured by the vertically oriented b_1 beam.
2) In Eq. (3) $(W)_{\text{True}}$ appears in the second term for the $(U)_{\text{True}}$ solution. The second term makes a correction for the effect of $(W)_{\text{True}}$ on $\mathbf{V}_2$.
3) The correction term is amplified by the cotangent of the oblique beam angle Θ. For $\Theta = 15°$, $\cot(15°) = 3.73$ and $\sec(15°) = 3.86$. For $\Theta = 30°$, $\cot(30°) = 1.73$ and $\sec(30°) = 2$.

b. Equations for a turbulent velocity field

Consider a turbulent fluid where $(W)_{\text{True}}$ and $(U)_{\text{True}}$ can be expressed in terms of average $(\bar{\ })$ and perturbation $(')$ values. Over the b_1 and b_2 beams, $(\overline{W} + w')_{\text{True}}$ will be denoted by $W_1 = \overline{W_1} + w_1'$ and $\mathbf{W}_2 = \overline{W_2} + w_2'$, respectively, where $\overline{W_1} = \overline{W_2} = 0$. The $(\overline{U} + u')_{\text{True}}$ over the b_2 beam will be denoted by $\overline{U_2} + u_2'$, where $\overline{U_2} > 0$ will be assumed. To characterize a retrieval algorithm for these turbulent conditions, consider the following revised formulation of the profiler observations:

$$\mathbf{V}_1 = w_1', \tag{4}$$

$$\mathbf{V}_2 = (\overline{U}_2 + u_2')_{\text{True}} \sin(\Theta) + w_2' \cos(\Theta). \tag{5}$$

The appropriate solution for the true horizontal velocity would be

$$(\overline{U}_2 + u_2')_{\text{True}} = \mathbf{V}_2 \sec(\Theta) - w_2' \cot(\Theta). \tag{6}$$

However, in general, w_2' is not observed. It is approximated by w_1', as in the following equation for the retrieved horizontal velocity:

$$(\overline{U}_2 + u_2')_{\text{Ret}} = \mathbf{V}_2 \sec(\boldsymbol{\Theta}) - w_1' \cot(\boldsymbol{\Theta}). \tag{7}$$

Note that $(\overline{U}_2 + u_2')_{\text{Ret}}$ can be expressed as the true horizontal velocity, $(\overline{U}_2 + u_2')_{\text{True}}$, plus an error term, by combining Eqs. (6) and (7):

$$(\overline{U}_2 + u_2')_{\text{Ret}} = (\overline{U}_2 + u_2')_{\text{True}} + (w_2' - w_1') \cdot \cot(\Theta). \tag{8}$$

The error term in (8) is composed of the difference between the perturbation vertical velocities from the two beams, amplified by the cotangent (Θ) factor. A similar error term appears for a profiler configuration with opposing oblique beams and no vertical beam [see Lu and Lueck (1999a), the first two terms on the rhs of their Eq. (3)]. It is useful to note that an error term would also exist in (8) for a retrieval algorithm that did not correct for w_1' in (7). Measurement errors and noise in $\mathbf{V}_1$ and $\mathbf{V}_2$ would generate additional error terms. Note that $(\overline{U}_2 + u_2')_{\text{Ret}}$ will be affected by the error term because turbulent eddies cause the vertical velocity to vary rapidly in time and space, resulting in $w_2' \neq w_1'$. As a result, $(\overline{U}_2 + u_2')_{\text{Ret}}$ can be expected to be more variable than $(\overline{U}_2 + u_2')_{\text{True}}$. However, $(\overline{U}_2 + u_2')_{\text{Ret}}$ will be unbiased with respect to $(\overline{U}_2 + u_2')_{\text{True}}$ if $w_2' - w_1'$ is zero and if variations in the error term are uncorrelated with $(u_2')_{\text{True}}$.

On the other hand, $(U_n^{\Delta})_{\text{Ret}}$ may be positively biased if positive peaks in the error term coincide with peak or near-peak values in $(\overline{U}_2 + u_2')_{\text{True}}$. The probability of such a coincidence would increase under one or more of the following three conditions: 1) as the averaging interval becomes long, 2) as the time scale of w' variations becomes short compared to the time interval between observations, and 3) as the distance between the beams becomes large compared to the spatial scale of the turbulent eddies. Some quantitative insights into these potential errors of $(U_n^{\Delta})_{\text{Ret}}$ can be obtained by use of a statistical model, as described in section 3, to simulate Doppler profiler observations and the resulting $(\overline{U}_2 + u_2')_{\text{Ret}}$.

c. Equations for a sinusoidal pattern in vertical velocity

A sinusoidal pattern in vertical velocity, as might be associated with waves within the atmosphere or ocean, would also contribute to errors in the retrieved horizontal velocity. Consider briefly the case where the vertical velocity can be described as $w(x) = A \cdot \sin(x/L)$. In this case x is a horizontal distance in the plane of the vertical and oblique beams at the level where the radial velocities $\mathbf{V}_1$ and $\mathbf{V}_2$ are measured, L determines the horizontal wavelength of the pattern, and A is its am-

plitude. Let x_1 and x_2 denote the horizontal coordinates of the vertical and oblique beams, respectively. The error in the retrieved horizontal velocity can now be expressed as

$$A[\sin(x_2/L) - \sin(x_1/L)]\cot(\Theta). \quad (9)$$

In the case where the sinusoidal pattern of vertical velocity was propagating across the profiler, the error term shown in (9) would also vary sinusoidally at a rate that was dependent on the distance between the beams, the wavelength of the pattern, and its speed of propagation. In general the retrieved horizontal velocity would have alternating positive and negative errors, resulting again in a positive bias of the peak horizontal velocity. The resulting error structure would have a complex dependence on altitude, the 3D propagation characteristics of the pattern, and its amplitude. While additional insights may be obtainable by a spectral formulation of the problem, further analysis is beyond the scope of the present effort.

3. Statistical modeling of peak horizontal velocity bias

The idealized profiler concept introduced in section 2b will be used here to obtain quantitative insights into the statistics of $(U_n^{\Delta})_{\text{True}}$ and $(U_n^{\Delta})_{\text{Ret}}$ by employing analytical properties of the type-I extreme value distribution for maxima (the Gumbel distribution).

A Gumbel distribution can be obtained by generating random samples of size n from a normal distribution, then extracting the maximum value from each sample and repeating the process ad infinitum (Coles 2001). The maxima will have a Gumbel distribution. In the present case, $(\overline{U_2} + u_2')_{\text{True}}$ is assumed to be normally distributed about $\overline{U_2}$, with a standard deviation of σ (Mitsuta and Tsukamoto 1989). In a thought experiment we imagine that from each random sample of size n from the population of $(\overline{U_2} + u_2')_{\text{True}}$, the peak, or maximum, value is selected and used to create a population of $(U_n^{\Delta})_{\text{True}}$. The distribution of $(U_n^{\Delta})_{\text{True}}$ will be Gumbel in form, with scale and location parameters λ_{True} and ξ_{True}, respectively. At the same time, a sample of $(\overline{U_2} + u_2')_{\text{Ret}}$ is generated consisting of $(\overline{U_2} + u_2')_{\text{True}}$ plus the random error term as described by (8). The error term comes from independent normal distributions of w_2' and w_1' with zero means and equal variances. A corresponding distribution of $(U_n^{\Delta})_{\text{Ret}}$ is generated by taking the maximum $(\overline{U_2} + u_2')_{\text{Ret}}$ for each sample of size n. When the error term is normally distributed and independent of $(\overline{U_2} + u_2')_{\text{True}}$, the resulting distribution of $(U_n^{\Delta})_{\text{Ret}}$ will also be Gumbel in form with parameters λ_{Ret} and ξ_{Ret}. The equations below describe how λ_{True}, ξ_{True}, λ_{Ret}, and ξ_{Ret} depend on n, $\overline{U_2}$, σ, and parameters of the error term. The error term will have a variance that depends on properties of $(w_2' - w_1')$ and the amplifying $\cot(\Theta)$ factor.

The Gumbel probability density function is given by

$$G(U^{\Delta}) = 1/\lambda \exp[-(U^{\Delta} - \xi)/\lambda] \exp\{-\exp[-(U^{\Delta} - \xi)/\lambda]\}. \quad (10)$$

The average value and variance of the maxima, U^{Δ} in this case, are given by

$$\overline{(U^{\Delta})} = \xi + 0.5772\lambda \text{ and} \quad (11)$$

$$\text{var}[U^{\Delta}] = (\pi^{2/6})\lambda^2, \quad (12)$$

respectively. The value 0.5772 is an approximation of Euler's constant (Abramowitz and Stegun 1965), hereafter Eu.

When $\overline{U_2}$ and σ_{True} are the mean and standard deviation of $(\overline{U_2} + u_2')_{\text{True}}$, the parameters of the resulting Gumbel probability density function (PDF) of $(U_n^{\Delta})_{\text{True}}$ are

$$\xi_{\text{True}} = \overline{U_2} + a_n\sigma_{\text{True}} \text{ and} \quad (13)$$

$$\lambda_{\text{True}} = b_n\sigma_{\text{True}}, \quad (14)$$

where a_n and b_n, known as normalizing constants, are dependent on the sample size and are given by (T. Rolf Turner, University of New Brunswick, 2003, personal communication)

$$a_n = \sqrt{[2\ln(n)]} - \{\ln(4\pi) + \ln[\ln(n)]\}/\{2\sqrt{[2\ln(n)]}\}. \quad (15)$$

$$b_n = 1/\sqrt{[2\ln(n)]}. \quad (16)$$

The average value of $(U_n^{\Delta})_{\text{True}}$ can then be written in terms of parameters of the underlying normal distribution and the normalizing constants by

$$\overline{(U_n^{\Delta})_{\text{True}}} = \overline{U_2} + \sigma_{\text{True}} \cdot (a_n + \text{Eu}b_n). \quad (17)$$

The $(a_n + \text{Eu}b_n)$ factor, hereafter G_C, is weakly dependent on n, changing from 2.56 to 2.92 as n goes from 100 to 300. For example, consider $\overline{U_2} = 10$, $\sigma_{\text{True}} = 2.0$, and $n = 100$. We find $\overline{(U_n^{\Delta})_{\text{True}}} = 15.1$.

Gumbel distribution parameters for $(U_n^{\Delta})_{\text{Ret}}$ are found by making use of (8) in section 2b. The variance of $(\overline{U_2} + u_2')_{\text{Ret}}$ will be affected by the error term, due to variance of $(w_2' - w_1')$ and the covariance of $(\overline{U_2} + u_2')$ with $(w_2' - w_1')$. The problem of solving for the variance of $(\overline{U_2} + u_2')_{\text{Ret}}$ and for the Gumbel parameters of $(U_n^{\Delta})_{\text{Ret}}$ can be simplified by assuming that the covariance between $(\overline{U_2} + u_2')$ and $(w_2' - w_1')$ is zero. That is, the difference in vertical velocities over the b_1 and b_2 beams is assumed to be uncorrelated with perturbations in the horizontal velocity. This assumption will be made, causing the variance of $(\overline{U_2} + u_2')_{\text{Ret}}$ to be greater than that of $(\overline{U_2} + u_2')_{\text{True}}$. It is the increased variance of $(\overline{U_2} + u_2')_{\text{Ret}}$ that results in a positive bias in $\overline{(U_n^{\Delta})_{\text{Ret}}}$.

The additional variance in $(\overline{U_2} + u_2')_{\text{Ret}}$ will be dependent on the variance of the difference in vertical

velocities over the two beams, $(w_2' - w_1')$. The variance of this difference will be referred to as the variance of the residual, var[Resid], because it could be zero if the vertical velocities over the two beams were identical. In the case where w_2' is known, the retrieval equation will not include the error term.

The variance of $(\overline{U_2} + u_2')_{\text{Ret}}$, var$[U_{\text{Ret}}]$, is then obtained by summing the variance of $(\overline{U_2} + u_2')_{\text{True}}$, or σ^2_{True}, with the product of var[Resid] and the square of the amplifying cotangent term:

$$\text{var}[U_{\text{Ret}}] = \sigma^2_{\text{True}} + \text{var[Resid]} \cdot \cot^2(\Theta). \quad (18)$$

For the case where var[Resid] $\cdot$ is $(1.0)^2$, $\Theta = 15°$, and the variance of $(\overline{U_2} + u_2')_{\text{True}}$ is $(2.0)^2$, var$[U_{\text{Ret}}]$ becomes 17.9, a substantial increase.

The average value for the $(U_n^{\Delta})_{\text{Ret}}$ can now be calculated from

$$\overline{(U_n^{\Delta})_{\text{Ret}}} = \overline{U_2} + \sigma_{\text{Ret}} G_c, \quad (19)$$

where $\sigma_{\text{Ret}} = \{\text{var}[U_{\text{Ret}}]\}^{1/2}$. From (19) we find $\overline{(U_n^{\Delta})_{\text{Ret}}} = 20.8$, using $\overline{U_2} = 10$, $\sigma^2 = 4.0$, and $n = 100$, as above; and $\overline{(U_n^{\Delta})_{\text{Ret}}}$ is ~38% higher than $\overline{(U_n^{\Delta})_{\text{True}}}$, which was found to be 15.1.

Figure 3 shows modeled PDFs of $(\overline{U_2} + u_2')_{\text{True}}$, $(U_n^{\Delta})_{\text{True}}$, and $(U_n^{\Delta})_{\text{Ret}}$ for the case outlined above. The $(U_n^{\Delta})_{\text{True}}$ and $(U_n^{\Delta})_{\text{Ret}}$ distributions are shifted significantly to the right of the underlying distribution of $(\overline{U_2} + u_2')_{\text{True}}$, because the theoretical peak value distributions were determined for sample sizes of 100. It is also evident that the distribution of $(U_n^{\Delta})_{\text{Ret}}$ is somewhat wider than that of $(U_n^{\Delta})_{\text{True}}$. For the case where $\Theta = 30°$, var$[U_{\text{Ret}}]$ would be reduced to 7.0 and the bias would be reduced to 11%. The bias decreases to zero as Θ approaches 90°, as expected.

The influence of the variance of $(w_2' - w_1')$ in enhancing $\overline{(U_n^{\Delta})_{\text{Ret}}}$ above $\overline{(U_n^{\Delta})_{\text{True}}}$ can be visualized by graphing the percent bias of $\overline{(U_n^{\Delta})_{\text{Ret}}}$ in a two-dimensional, normalized coordinate system of $\sigma_{\text{True}}/\overline{U_2}$ versus $\sigma_{\text{Resid}}/\overline{U_2}$. Figure 4 shows contours of the percent bias,

$$\%\text{Bias} = 100[\overline{(U_n^{\Delta})_{\text{Ret}}} - \overline{(U_n^{\Delta})_{\text{True}}}]/\overline{(U_n^{\Delta})_{\text{True}}} \quad (20)$$

for the case where $n = 100$ and $\Theta = 15°$. The greatest bias is found when the residual variance in vertical velocity is large compared to the variance in horizontal velocity. The bias becomes small when the residual variance in vertical velocity is small.

Figure 5 shows contours of the percent bias for the case where $n = 100$ and $\Theta = 30°$. For fixed values of $\sigma_{\text{Resid}}/\overline{U_2}$ and $\sigma_{\text{True}}/\overline{U_2}$, the percent bias with $\Theta = 30°$ is less than half that for $\Theta = 15°$ (Fig. 4) because of the strong Θ dependence of the $\cot^2(\Theta)$ factor.

4. Summary and conclusions

Numerous previous studies have shown that Doppler profilers are capable of providing accurate retrievals of average horizontal velocities in the atmosphere and underwater. However, estimates of peak horizontal velocities from collections of instantaneous retrievals are susceptible to a positive bias, due to turbulent vertical motions in the medium of interest.

An idealized Doppler profiler configuration was combined with a statistical model of normally distributed velocity fluctuations and a simple retrieval algorithm to illustrate the nature of the bias and its magnitude. The results revealed that unresolved vertical mo-

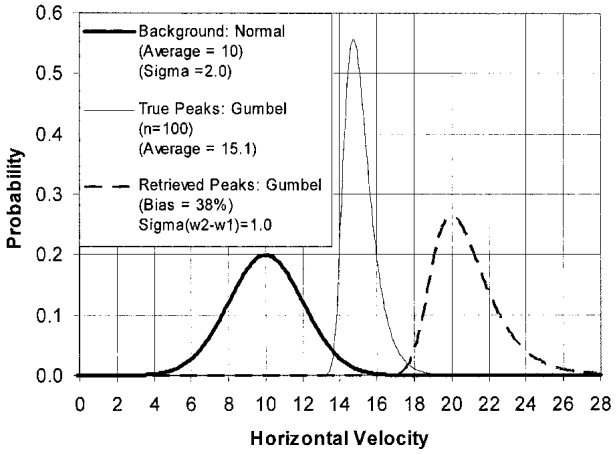

FIG. 3. Modeled PDFs of horizontal velocities illustrating Gumbel distributions of true and retrieved peaks derived from a background distribution that is Gaussian. Distribution parameters have been chosen to give an average background velocity of 10, an average value of 15.1 for the true peaks, and a bias of 38% for the retrieved peaks. The standard deviation of true horizontal velocities is 2.0 and that of the residual vertical velocity is 1.0.

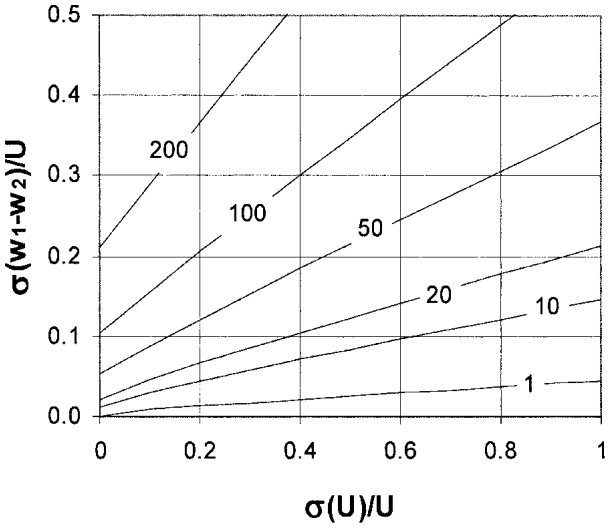

FIG. 4. The percent bias in $\overline{(U_n^{\Delta})_{\text{Ret}}}$ as a function of $\sigma_{\text{True}}/\overline{U}$ and $\sigma_{\text{Resid}}/\overline{U}$, for $n = 100$ and $\Theta = 15°$, based on the analytical models for horizontal and vertical velocity presented in section 3.

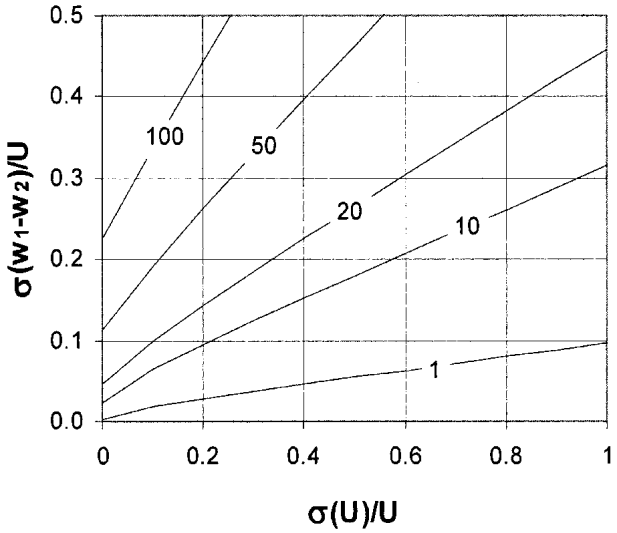

FIG. 5. As in Fig. 4, but for $\Theta = 30°$.

tions contaminate the instantaneous retrievals because of limitations inherent in the beam configuration of typical profilers. The retrieved instantaneous horizontal velocities are more variable than the true instantaneous velocities, resulting in a positive bias when the peak retrieved value is chosen.

The increased variability in the retrieved instantaneous horizontal velocities can be expressed by the sum of the true variability and an error term that depends only on the unresolved variance in the vertical velocity and the zenith angle of the oblique beams [see Eq. (18)]. This suggests that the percent bias may be reduced by assuming a lognormal distribution for the horizontal velocities, because extreme events occur more frequently than with a normal distribution (Merceret 1997). The true variability would increase while the error term would remain the same. However, an assumption of lognormality for vertical velocity variations may result in an increase in the error term.

The bias in average peak horizontal velocity can be characterized in terms of turbulent properties of the flow. Errors in the measurement of the vertical velocity and instrumental noise would also contribute to the bias. These findings suggest that an average correction could be applied to the retrieved peak values. However, the correction would be statistical in nature and would not necessarily improve the precision of individual retrieved peak values.

Acknowledgments. The authors thank Ms. Winifred Lambert and Dr. Greg Taylor for their useful comments on this project. Mention of a copyrighted, trademarked or proprietary product, service, or document does not constitute endorsement thereof by the author, ENSCO, Inc., the AMU, the National Aeronautics and Space Administration, or the U.S. government. Any such mention is solely to inform the reader of the resources used to conduct the work reported herein.

APPENDIX

List of Symbols

a_n	Gumbel normalizing constant
b_n	Gumbel normalizing constant
b_1 beam	Vertical beam
b_2 beam	Oblique beam
D_1	Distance along b_1-beam axis
D_2	Distance along b_2-beam axis
Eu	Euler's constant
G_C	Gumbel constant $[a_n+b_n(\text{Eu})]$
$G(x)$	Gumbel probability density function
H	Height above the profiler
n	Sample size
p	Location of profiler
Resid	Residual quantity
R	Radial velocity
r'	Perturbation R
U	Horizontal velocity
u'	Perturbation horizontal velocity
var $[x]$	Variance of the variable x
$\mathbf{V}_1$	Radial velocity along b_1-beam axis
$\mathbf{V}_2$	Radial velocity along b_2-beam axis
W	Vertical velocity
w'	Perturbation vertical velocity
Θ	Angle between vertical and oblique beams
λ	Scale parameter for Gumbel distribution
ξ	Location parameter for Gumbel distribution
σ	Standard deviation
$\bar{}$	Overbar indicates ensemble average value
$'$	Prime indicates perturbation value
Δ	Indicates a peak value
1	Subscript 1 indicates vertical beam
2	Subscript 2 indicates oblique beam
Ret	Subscript Ret indicates a retrieved value
True	Subscript True indicates a true value

REFERENCES

Abramowitz, M., and I. A. Stegun, 1965: *Handbook of Mathematical Functions*. Dover, 1046 pp.

Chereskin, T. K., D. Halpern, and L. A. Regier, 1987: Comparison of shipboard acoustic Doppler current profiler and moored current measurements in the equatorial Pacific. *J. Atmos. Oceanic Technol.,* **4,** 742–747.

Coles, S., 2001: *An Introduction to Statistical Modeling of Extreme Values*. Series in Statistics, Vol. XIV, Springer, 208 pp.

Crescenti, G. H., 1997: A look back on two decades of Doppler sodar comparison studies. *Bull. Amer. Meteor. Soc.,* **78,** 651–673.

Gilboy, T. P., T. D. Dickey, D. E. Sigurdson, X. Yu, and D. Manov, 2000: An intercomparison of current measurements using a vector measuring current meter, an acoustic Doppler current profiler, and a recently developed acoustic current meter. *J. Atmos. Oceanic Technol.,* **17,** 561–574.

Kramar, V. F., and R. D. Kouznetsov, 2002: A new concept for

estimation of turbulent parameter profiles in the ABL using sodar data. *J. Atmos. Oceanic Technol.,* **19,** 1216–1224.

Lu, Y., and R. G. Lueck, 1999a: Using a broadband ADCP in a tidal channel: Part I: Mean flow and shear. *J. Atmos. Oceanic Technol.,* **16,** 1556–1567.

——, and ——, 1999b: Using a broadband ADCP in a tidal channel: Part II: Turbulence. *J. Atmos. Oceanic Technol.,* **16,** 1568–1579.

May, P. T., T. Sato, M. Yamamoto, S. Kato, T. Tsuda, and S. Fukao, 1989: Errors in the determination of wind speed by Doppler radar. *J. Atmos. Oceanic Technol.,* **6,** 235–242.

Merceret, F. J., 1997: Risk assessment consequences of the log-normal distribution of midtropospheric wind changes. *J. Spacecr. Rockets,* **35,** 111–112.

Mitsuta, Y., and O. Tsukamoto, 1989: Studies on spatial structure of wind gust. *J. Appl. Meteor.,* **28,** 1155–1160.

Peterson, V. L., 1988: Wind profiling: The history, principles, and applications of clear-air Doppler radar. Tycho Technology, 66 pp.

Short, D. A., and M. M. Wheeler, 2003: MiniSODAR evaluation. NASA Contractor Rep. NASA/CR-2003-211192, Kennedy Space Center, FL, 34 pp. [Available from ENSCO, Inc., 1980 N. Atlantic Ave., Suite 230, Cocoa Beach, FL 32931.]

Van Zandt, T. E., 2000: A brief history of the development of wind-profiling or MST radars. *Ann. Geophys.,* **18,** 740–749.

Woodward, W. E., and G. F. Appell, 1986: Current velocity measurements using acoustic Doppler backscatter: A review. *IEEE J. Oceanic Eng.*, **OE-11,** 3–6.